

Hydrogen Abstraction Reactions of OH Radicals with $\text{CH}_3\text{CH}_2\text{CH}_2\text{Cl}$ and $\text{CH}_3\text{CHClCH}_3$: A Mechanistic and Kinetic Study

Li Wang,^[a] Yanjie Li,^[a] Hongqing He,^[b] and Jinglai Zhang^{*[a]}

The hydrogen abstraction reactions of OH radicals with $\text{CH}_3\text{CH}_2\text{CH}_2\text{Cl}$ (R1) and $\text{CH}_3\text{CHClCH}_3$ (R2) have been investigated theoretically by a dual-level direct dynamics method. The optimized geometries and frequencies of the stationary points are calculated at the B3LYP/6-311G(d,p) level. To improve the reaction enthalpy and potential barrier of each reaction channel, the single point energy calculation is performed by the BMC-CCSD method. Using canonical variational transition-state theory (CVT) with the small-curvature tunneling correction, the rate constants are evaluated over a wide temperature range of 200–2000 K at the BMC-CCSD//B3LYP/6-311G(d,p) level. For the reaction channels with the negative barrier heights, the rate constants are calculated by using the CVT. The calculated total rate constants are consistent with available experimental data. The

results show that at lower temperatures, the tunneling correction has an important contribution in the calculation of rate constants for all the reaction channels with the positive barrier heights, while the variational effect is found negligible for some reaction channels. For reactions OH radicals with $\text{CH}_3\text{CH}_2\text{CH}_2\text{Cl}$ (R1) and $\text{CH}_3\text{CHClCH}_3$ (R2), the channels of H-abstraction from $-\text{CH}_2-$ and $-\text{CHCl}$ groups are the major reaction channels, respectively, at lower temperatures. With temperature increasing, contributions from other channels should be taken into account. Finally, the total rate constants are fitted by two models, i.e., three-parameter and four-parameter expressions. The enthalpies of formation of the species $\text{CH}_3\text{CHClCH}_2$, $\text{CH}_3\text{CHCH}_2\text{Cl}$, and $\text{CH}_2\text{CH}_2\text{CH}_2\text{Cl}$ are evaluated by isodesmic reactions. © 2011 Wiley Periodicals, Inc. *J Comput Chem* 33: 66–75, 2012

Keywords: $\text{CH}_3\text{CH}_2\text{CH}_2\text{Cl}$ · $\text{CH}_3\text{CHClCH}_3$ · Rate constants · Direct dynamics method · Four-parameter expression

Introduction

Chlorinated organic compounds are widely used in different industries. Once they are diffused into the stratosphere, these compounds will be potential sources of chlorine atoms which may initiate the chain destruction of ozone. The gas-phase oxidation is an important sink for the chloroalkanes in the troposphere and is thought to be dominated by reactions with OH radicals as their reactions with O_3 and NO_3 as well as their photolysis are negligible.^[1–3] Assessment of the impact of these chloroalkanes on the atmospheric environment requires accurate kinetic and mechanistic data over appropriate ranges of temperature. Although a broad kinetic data are available for the reactions of OH radicals with pure hydrocarbons^[4,5] and to a lesser extent for reactions with haloalkanes,^[6,7] there are limited reports on the reactions including more than two carbon atoms, particularly for the temperature-dependence rate constants. Reactions $\text{CH}_3\text{CH}_2\text{CH}_2\text{Cl} + \text{OH}$ (R1) and $\text{CH}_3\text{CHClCH}_3 + \text{OH}$ (R2) have been studied by three groups; k_1 and k_2 were measured at 303 K by Donaghy et al.^[8] and in the temperature ranges of 295–353 K and 233–372 K by Markert and Nielsen^[9] and Mu and Mellouki,^[10] respectively. For the reaction R1, the rate constants reported by the three groups can be considered in agreement allowing for the experimental uncertainties. However, the value of k_2 obtained by Donaghy et al.^[8] ($9.2 \pm 2.3 \times 10^{-13} \text{ cm}^3 (\text{mol s})^{-1}$ at 303 K, is almost two times higher than that reported by Markert and Nielsen.^[9] The value

measured by Mu and Mellouki^[10] is between two aforementioned results. Moreover, the rate constant at room temperature obtained by Mu and Mellouki^[10] agrees well with the value estimated by using the structure-reactivity approach proposed and extended by Atkinson.^[11,12] In these experimental and theoretical studies, only the total rate constants were reported while the detailed mechanism as well as the branching ratio was not discussed. The aim of this work is to give a deep insight into the mechanism of multichannel reactions


[a] L. Wang, Y. Li, J. Zhang

Institute of Environmental and Analytical Sciences, College of Chemistry and Chemical Engineering, Henan University, Kaifeng, Henan 475004, People's Republic of China

[b] H. He

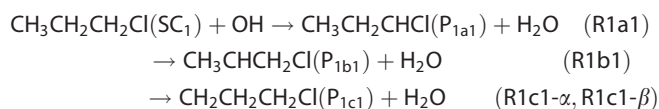
Wuhan Center for Magnetic Resonance, State Key Laboratory of Magnetic Resonance and Atomic and Molecular Physics, Wuhan Institute of Physics and Mathematics, Chinese Academy of Sciences, Wuhan 430071, People's Republic of China
E-mail: zhangjinglai@henu.edu.cn

Contract/grant sponsor: National Natural Science Foundation of China; Contract/grant numbers: 21003036; Contract/grant sponsor: Science Foundation of Henan Province; Contract/grant numbers: 2008A150005, 2011B150003; Contract/grant sponsor: Science Foundation of Henan University; Contract/grant numbers: 2009YBZR013, SBJ090507; Contract/grant sponsor: Doctor Foundation of Henan University

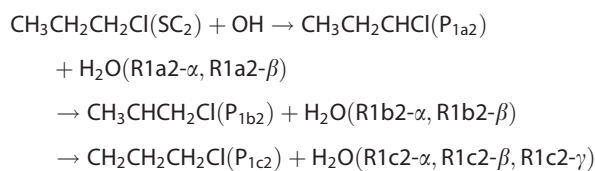
 Additional Supporting Information may be found in the online version of this article.

CH₃CH₂CH₂Cl and CH₃CHClCH₃ with OH radicals as well as to provide the temperature dependence of rate constants over a wide temperature range.

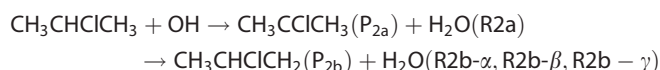
For the molecule CH₃CH₂CH₂Cl, there are two stable conformers, SC₁ and SC₂ with C_s and C₁ symmetry, respectively. Based on calculation, SC₂ is only stabler than SC₁ by 0.08 kcal mol⁻¹ at the BMC-CCSD//B3LYP/6-311G(d,p) level. So, these two conformers have similar stability and will both contribute to the overall rate constants. Due to the C_s symmetry of SC₁ structure, the hydrogen atoms in the -CH₂- and -CH₂Cl group are equivalent, denoted by the corresponding channels R1a and R1b; for the three hydrogen atoms in the -CH₃ group, two of them is equivalent and the third one is different from them with the corresponding reaction channels R1c-α and R1c-β. These channels are defined as follows:



As for the SC₂ with C₁ symmetry, each hydrogen atom is not equivalent, and as a result, seven distinguishable channels are found according to the different position of these seven H-atoms, that is,



As to the reactant CH₃CHClCH₃, hydrogen atom can be abstracted from -CHCl- group (denoted as channel R2a) and -CH₃ group (denoted as channel R2b). The three hydrogen atoms located in the -CH₃ group are different, so three distinct reaction channels are found for reaction R2b (denoted as channels R2b-α, R2b-β, and R2b-γ), that is,

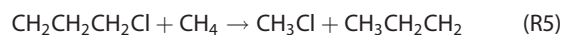
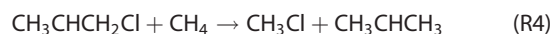
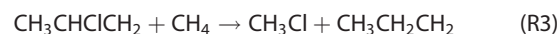


As a result of C_s symmetry of the molecule CH₃CHClCH₃, both -CH₃ groups are the equivalent, and hydrogen channels R2b-α, R2b-β, R2b-γ are the same for the other -CH₃ group.

Here, a dual-level approach (X/Y)^[13-17] is used to study the kinetic nature of the reactions over a wide temperature range. In this methodology, the potential energy information can be calculated directly from a sufficiently accurate molecular orbital theory only in the region of configuration space along a reaction path, without the intermediary of a potential surface fit. As usual, dual-level X/Y refers to optimization and frequencies calculated at lower-level Y with single-point energies calculated at higher-level X. Here, the electronic structure information is obtained directly from density functional theory (DFT) calculations. Then, single-point energies are calculated by BMC-CCSD method based on the lower level DFT geometries. Subsequently, by means of the Polyrate 9.7 program,^[18]

the rate constants are calculated using the variational transition-state theory (VTST) proposed by Truhlar and co-workers.^[19-21] The theoretical and experimental results are compared. Furthermore, the temperature dependence of the rate constants and the branching ratios are discussed.

In addition, the enthalpies of formation of CH₃CHClCH₂, CH₃CHCH₂Cl, and CH₂CH₂CH₂Cl radicals are estimated by the following isodesmic reactions:



Calculation Methods

All electronic structure calculations involved in this work are completed by the Gaussian 09 program package.^[22] The geometries and frequencies of all the stationary points (including reactants, complexes, products, and transition states) of two reactions are calculated by Becke's three-parameter nonlocal-exchange functional with the nonlocal correlation of Lee-Yang-Parr method (B3LYP)^[23,24] using the 6-311G(d,p) basis set. To get more reliable reaction energy and barrier height, single-point corrections are performed by BMC-CCSD theory^[25] using the B3LYP -optimized geometries. Furthermore, the effect of the basis set superposition error (BSSE) on the energies of complexes is considered by means of the counterpoise method proposed by Boys and Bernardi.^[26] To check the reliability of the results obtained at the B3LYP/6-311G(d,p) level, the stationary geometries of reaction channels R1b1, R1b2-β, and R2a are optimized using the B3LYP functional with the 6-311+G(d,p) basis set and the BMK (Boese-Martin for Kinetics)^[27] functional with the 6-311G(d,p) and 6-311+G(d,p) basis sets. To yield more reliable barrier heights, single-point calculations for above reaction channels are performed at other two higher levels, i.e., MCG3-MPWPW91^[28] and MCQCISD-MPWPW91^[28] methods. We tested various single-point methods based on the different optimized geometries, respectively. The harmonic vibrational frequencies are calculated to characterize the nature of each critical point and to make zero-point-energy correction. Transition states (TSs) show only one negative eigenvalue in their diagonalized force constant matrices, and their associated eigenvectors are confirmed to correspond to the motion along the reaction coordinate under consideration, using the intrinsic reaction coordinate (IRC) method. Also, first and second energy derivatives at geometries along the MEP are obtained to calculate the curvature of the reaction path and the generalized vibrational frequencies along the reaction path. The dual-level potential profile along the reaction path is further refined with the interpolated single-point energies (ISPE) method,^[29] in which a few extra single-point calculations are needed to correct the lower level reaction path.

The information on the potential energy surface is used to evaluate the rate constants by means of the Polyrate 9.7

program. The rate constants are calculated by using the VTST^[19–21] proposed by Truhlar and co-workers. The specific level of VTST that we used is canonical variational transition-state theory (CVT)^[30–32] with the small-curvature tunneling (SCT)^[33,34] method. The two electronic states for OH radicals, with a 140 cm⁻¹ splitting in the ²II ground state, are included in calculating its electronic partition functions. The curvature components are calculated by using a quadratic fit to obtain the derivative of the gradient with respect to the reaction coordinate.

Results and Discussion

Stationary points

The geometric parameters of all the reactants, complexes, TSs, and products are optimized at the B3LYP/6-311G(d,p) level. Owing to the similarity, only the optimized structures of the reactants and TSs involved in the channels R1a (including channels R1a1 and R1a2- α), R1b (including R1b1 and R1b2- β), R1c (including R1c1- β and R1c2- β), R2a, and R2b- β as the representatives of H-abstraction from each group are shown in Figure 1. The geometric parameters of other stationary points including the TSs, complexes, and products are presented in Supporting Information (Fig. S1). It is seen that the theoretical values are in reasonable agreement with the experimental values^[35–38] to within the maximum error of 2%. In addition, owing to the electronegativity of the oxygen atom and chlorine atom, hydrogen-bonded complexes are found at the entrance or exit channels of reactions R1 and R2. As shown in Figure 1, two stable conformers of CH₃CH₂CH₂Cl, SC₁ and SC₂, are located. Conformers SC₁ and SC₂ mean that Cl atom lies in and out of the C-C-C plane with C_s and C₁ symmetry, respectively. Because of SC₁ with C_s symmetry, four TSs are found for the reaction CH₃CH₂CH₂Cl(SC₁) with OH radical and they are labeled as TS_{1a1}, TS_{1b1}, TS_{1c1- α} and TS_{1c1- β} . However, for the reaction CH₃CH₂CH₂Cl(SC₂) with OH radical, seven TSs are located according to seven different hydrogen positions and they are designated as TS_{1a2- α} , TS_{1a2- β} , TS_{1b2- α} , TS_{1b2- β} , TS_{1c2- α} , TS_{1c2- β} and TS_{1c2- γ} . In the TSs TS_{1a1} and TS_{1a2- γ} corresponding to the H-abstraction from -CH₂Cl group in SC₁ and SC₂, the breaking bond C-H is elongated by 6.5% and 7.3% compared with the equilibrium C-H bond length in isolated reactants; and the forming bond O-H is elongated by 51% and 48% compared with the equilibrium bond length in isolated H₂O molecule, respectively. When hydrogen is abstracted from -CH₂- and -CH₃ groups, i.e., channels R1b and R1c, the corresponding TSs show the similar character as displayed in Figure 1 and Figure S1. Based on above analysis, it is easy to conclude that the geometries of TSs involved in H-abstraction from the same groups of SC₁ and SC₂ are similar. One stable conformer of CH₃CHClCH₃ is found with C_s symmetry and thus, two -CH₃ groups are equivalent. Four TSs corresponding to hydrogen-abstraction channels are found for the reaction CH₃CHClCH₃ with OH radical and they are denoted as TS_{2a}, TS_{2b- α} , TS_{2b- β} and TS_{2b- γ} . With respect to the TSs TS_{2a} and TS_{2b- β} , the C-H bond, which is broken, is stretched by 3.7% and 12% com-

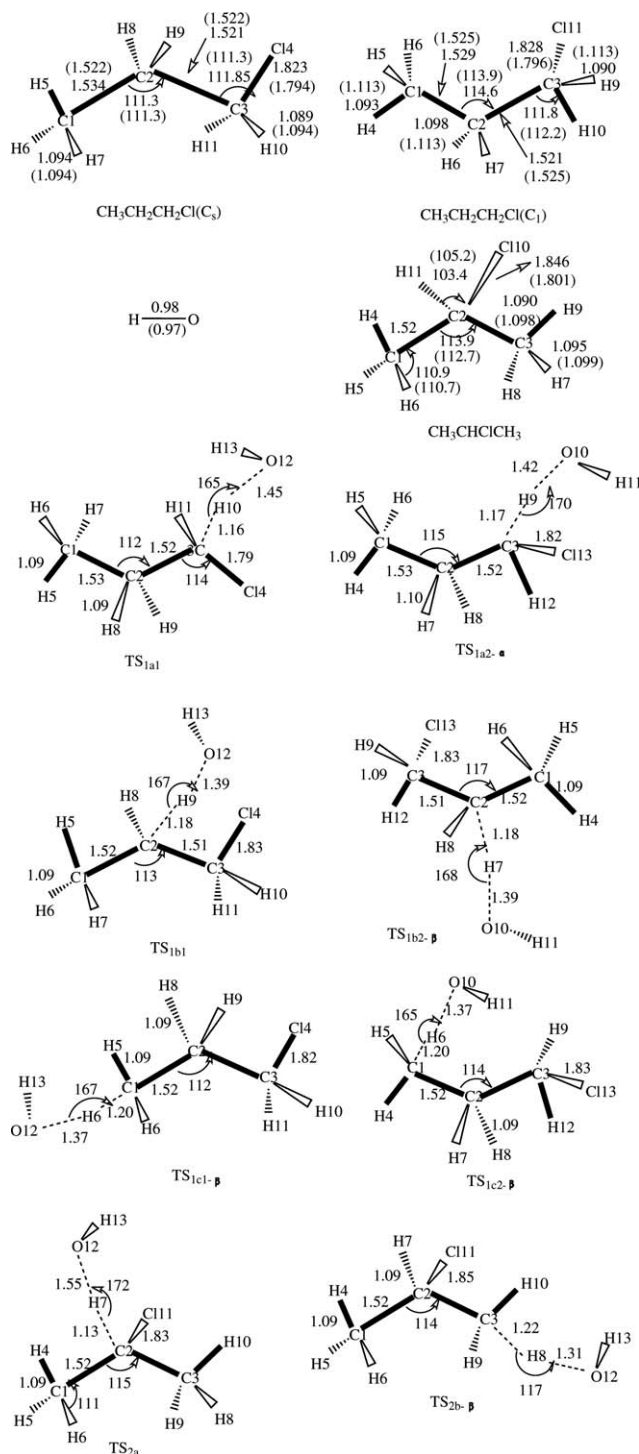


Figure 1. Optimized geometries of reactants and selected TSs at the B3LYP/6-311G(d,p) level. The values in the parentheses are the experimental values.^[35–38] Bond lengths are in angstroms and angles are in degrees.

pared with the C-H equilibrium bond length of CH₃CHClCH₃ and the O-H bond, which is formed, is longer than equilibrium bond length of H₂O by 61.5% and 36.5%, respectively. The elongation of the forming bond is much greater than that of the breaking bond, indicating that these TSs are reactant-like, i.e., all these reactions proceed via “early” TSs, as expected for exothermic reactions.

The harmonic vibrational frequencies are calculated at the same level of theory to characterize the nature of each critical point and to make zero-point energy (ZPE) correction. In the Supporting Information, the harmonic vibrational frequencies of all the reactants, complexes, products, and TSs along with the available experimental data^[37,38] are listed in Tables S1–S3. All of the minima including reactants, products, and complexes correspond to all real frequencies, but the TSs are confirmed to have only one imaginary frequency.

There are no available experimental enthalpies of formation (ΔH_{f298}^0) for CH₃CHCH₂Cl, CH₂CH₂CH₂Cl, and CH₃CHClCH₂ species involved in the title reactions. Thus, in this study, their ΔH_{f298}^0 values are estimated by using the isodesmic reactions R3–R5. As the number of electron pairs in the reactants and products are conserved in isodesmic reaction, the change in their correlation energies is usually small. So, the reaction energies of isodesmic reactions can be predicted quite accurately with relatively cheap theoretical method. Thus, isodesmic reaction is thought to be a useful tool to estimate the heats of formation of the unknown compounds. First, the reaction enthalpies of R3–R5 are calculated at the BMC-CCSD//B3LYP level. Second, these theoretical results are combined with the known enthalpies of formation (CH₄ –17.91 kcal mol⁻¹; CH₃Cl –20.02 kcal mol⁻¹; CH₃CHCH₃ 21.53 ± 0.48 kcal mol⁻¹; CH₃CH₂CH₂ 23.92 ± 0.48 kcal mol⁻¹)^[39,40] to estimate the required enthalpies of formation of target species at 298 K. The enthalpies of formation are 14.33 ± 0.48 kcal mol⁻¹ for CH₃CHCH₂Cl, 16.82 ± 0.48 kcal mol⁻¹ for CH₂CH₂CH₂Cl, and 13.95 ± 0.48 kcal mol⁻¹ for CH₃CHClCH₂. Note that the error limits are computed by adding the maximum uncertainties of ΔH_{f298}^0 values of the reference compounds taken from the literature.

The reaction enthalpies (ΔH_{298}^0) for the two reactions calculated at the B3LYP/6-311G(d,p) and BMC-CCSD//B3LYP/6-311G(d,p) levels are listed in Table 1. It is shown that all the reactions are exothermic and the calculated reaction enthalpies are decreased by about 2–5 kcal mol⁻¹ when the BMC-CCSD method is used. Table 1 also shows that the values of ΔH_{298}^0 for reaction channels involved in H-abstraction from the same group are very close or the same. Thus, it is reasonable to choose the lowest reaction enthalpy to compare with the experimental value. The calculated enthalpies of –22.63 (R1a1), –22.62 (R1a2), and –23.80 (R2a) kcal mol⁻¹ at the higher level are in reasonable agreement with the experimen-

tal values of –21.46 ± 0.22 kcal mol⁻¹ for reaction channels R1a1 and R1a2 and –25.06 ± 1.3 kcal mol⁻¹ for reaction R2a, respectively, which is derived from the experimental standard heats of formation^[41–46] (OH, 8.85 kcal mol⁻¹; H₂O, –57.81 kcal mol⁻¹; CH₃CH₂CH₂Cl, –31.7 ± 0.22 kcal mol⁻¹; CH₃CH₂CHCl, 13.5 kcal mol⁻¹; CH₃CHClCH₃, –34.4 ± 1.2 kcal mol⁻¹; CH₃CClCH₃, 7.2 ± 0.1 kcal mol⁻¹). As the calculated enthalpies of the reactions R1a and R2a agree well with the experimental values, it can be inferred that the enthalpies of other reaction channels R1b, R1c, and R2b calculated at the same level are reliable.

Schematic potential energy profiles of three reactions with ZPE corrections are plotted in Figures 2a-1, 2a-2, and 2b. Note that the energy of reactants R is set to zero as a reference. The energies of some complexes are close to those of the corresponding reactants or products. On the contrary, the energy differences between some complexes and reactants or products are very large. So, one question arises: do these complexes really exist or is it an artifact due to the theoretical methods? To test the stability of the complexes, the BSSE correction is estimated using the counterpoise method. The energies of complexes with and without BSSE correction and the BSSE energies calculated at the BMC-CCSD level are listed in Table 2. The complexes CR_{1a1}, CR_{1b2- α} , and CR_{2b- γ} disappear when BSSE correction is included. For reaction R1, the barrier heights of reaction channel R1b are lower by about 1–3 kcal mol⁻¹ than the values of reaction channels R1a (including channels R1a1, R1a2- α , and R1a2- β) and R1c (including channels R1c1- α , R1c1- β , R1c2- α , R1c2- β , and R1c2- γ). Thus, it can be expected that for reaction R1, channel R1b (H-abstraction from –CH₂– group) is the major reaction channel. The barrier heights involved in the H-abstraction reaction channels from the same group are slightly different. For example, the barrier heights with ZPE corrections for reaction channels R1a1, R1a2- α , and R1a2- β , which are involved in the H-abstraction from the –CH₂Cl group, are 1.37, 0.40, and 0.60 kcal mol⁻¹, respectively, at the BMC-CCSD//B3LYP level, as shown in Figures 2a-1 and 2a-2. By analysis, we find that for channels R1a2- α and R1a2- β , the ring structure of TSs TS_{1a2- α} and TS_{1a2- β} leads to the decrease of barrier height. Similarly, for reaction CH₃CHClCH₃ with OH radical, due to the effect of the analogous ring structure, the barrier heights of channels R2b- α , R2b- β , and R2b- γ decrease in the order $\Delta E_{2b-\gamma}$ (1.90 kcal mol⁻¹) > $\Delta E_{2b-\alpha}$ (0.72 kcal mol⁻¹) > $\Delta E_{2b-\beta}$ (0.50 kcal mol⁻¹). The six-

Table 1. Enthalpies of reactions (in kcal mol⁻¹) at the B3LYP/6-311G(d,p) and BMC-CCSD//B3LYP/6-311G(d,p) levels and available experimental values.^[41–46]

Reactions	B3LYP/6-311G(d,p)	BMC-CCSD//B3LYP/6-311G(d,p)	Expt.
CH ₃ CH ₂ CH ₂ Cl (SC ₁)+OH→CH ₃ CH ₂ CHCl (P _{1a1})+H ₂ O (R1a1)	–17.13	–22.63	–21.46 ± 0.22
→CH ₃ CHCH ₂ Cl (P _{1b1})+H ₂ O (R1b1)	–19.64	–21.79	
→CH ₂ CH ₂ CH ₂ Cl (P _{1c1})+H ₂ O (R1c1)	–13.28	–18.43	
CH ₃ CH ₂ CH ₂ Cl(SC ₂)+OH→CH ₃ CH ₂ CHCl (P _{1a2-α})+H ₂ O(R1a2- α)	–17.04	–22.46	–21.46 ± 0.22
→CH ₃ CH ₂ CHCl (P _{1a2-β})+H ₂ O(R1a2- β)	–17.19	–22.62	
→CH ₃ CHCH ₂ Cl (P _{1b2})+H ₂ O (R1b2)	–19.70	–21.62	
→CH ₂ CH ₂ CH ₂ Cl (P _{1c2})+H ₂ O (R1c2)	–13.06	–18.52	
CH ₃ CHClCH ₃ +OH→CH ₃ CClCH ₃ (P _{2a})+H ₂ O (R2a)	–19.46	–23.80	–25.06 ± 1.3
→CH ₃ CHClCH ₂ (P _{2b})+H ₂ O (R2b)	–14.66	–17.99	

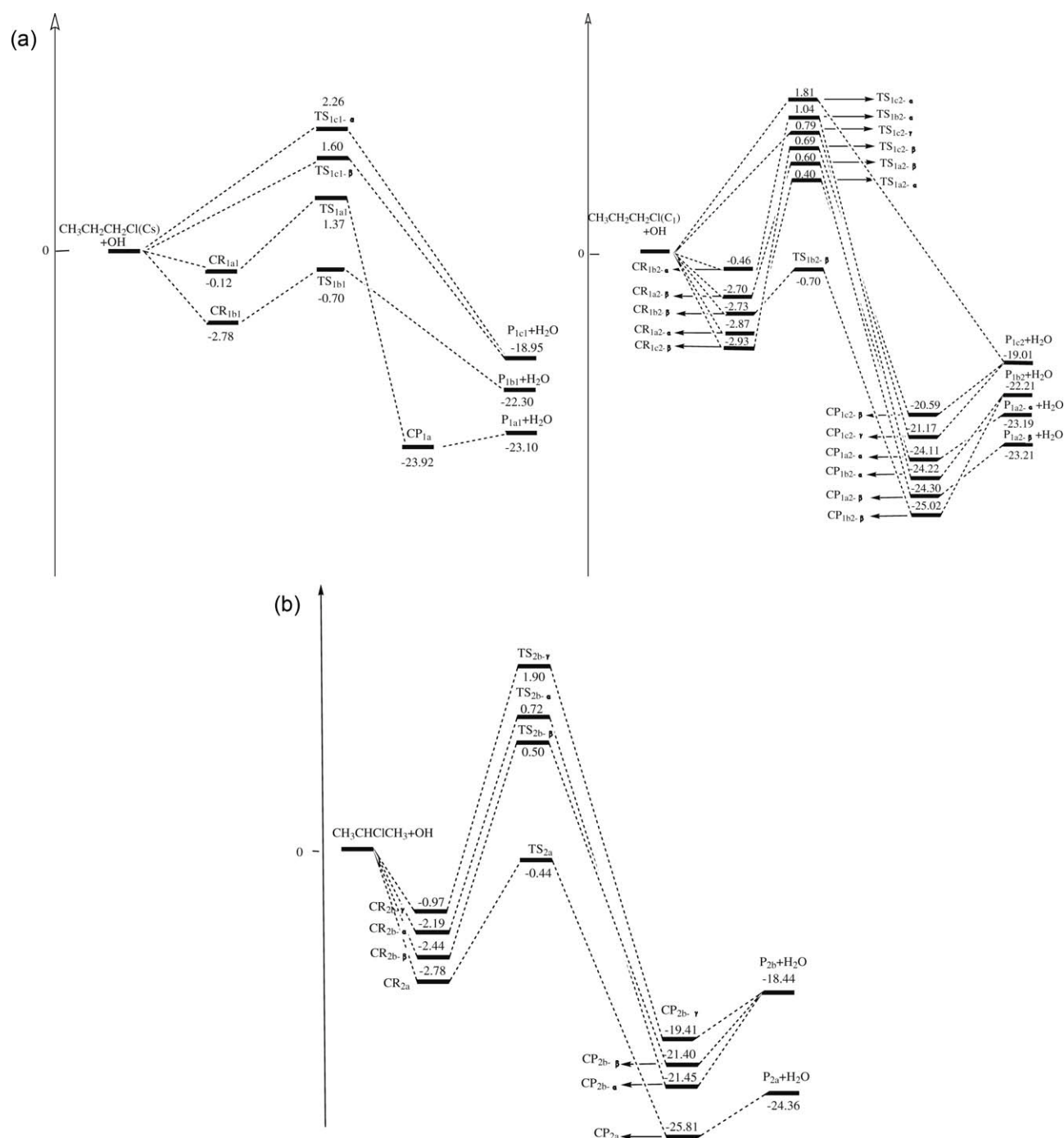


Figure 2. a-1) Schematic pathways for the reaction $\text{CH}_3\text{CH}_2\text{CH}_2\text{Cl}$ (SC_1) + OH. Relative energies with ZPE at the BMC-CCSD//B3LYP/6-311G(d,p) level are in kcal mol^{-1} . a-2) Schematic pathways for the reaction $\text{CH}_3\text{CH}_2\text{CH}_2\text{Cl}$ (SC_2) + OH. Relative energies with ZPE at the BMC-CCSD//B3LYP/6-311G(d,p) level are in kcal mol^{-1} . b) Schematic pathways for the reaction $\text{CH}_3\text{CHClCH}_3$ + OH. Relative energies with ZPE at the BMC-CCSD//B3LYP/6-311G(d,p) level are in kcal mol^{-1} .

member ring structure of TSs, $\text{TS}_{2b-\alpha}$ and $\text{TS}_{2b-\beta}$ results in the decrease of barrier height. For channel $\text{R}_{2b-\alpha}$, the hydrogen atom (H10) abstracted lies between Cl11 and H7, whereas for channel $\text{R}_{2b-\beta}$ the hydrogen atom (H8) abstracted lies behind Cl11 and H7; so, the steric hindrance for channel $\text{R}_{2b-\alpha}$ is little larger than that for channel $\text{R}_{2b-\beta}$. As to channel $\text{R}_{2b-\gamma}$, though the hydrogen atom (H9) abstracted lies behind Cl11 and H7, no six-member ring structure is formed in the TS $\text{TS}_{2b-\gamma}$.

Thus, the channel $\text{R}_{2b-\gamma}$ has the highest potential energy barrier. The six-member ring structure has a greater impact on the barrier comparing with the effect of the steric hindrance.

This reactivity based on the barrier heights is in line with the change of the dissociation energy (D_{298}^0) of C-H bond. For $\text{CH}_3\text{CH}_2\text{CH}_2\text{Cl}$ (including two conformers SC_1 and SC_2), we can see that at the BMC-CCSD//B3LYP level, the bond energy D_{298}^0 ($-\text{CH}_2\text{Cl}$) ($95.67 \text{ kcal mol}^{-1}$) is almost equal to D_{298}^0 ($-\text{CH}_2-$)

Table 2. Energies of complexes (in kcal mol^{-1}) calculated at the BMC-CCSD//B3LYP/6-311G(d, p) level.

	Without BSSE correction	BSSE energy	With BSSE correction
CR _{1a1}	-0.12	1.26	1.14
CR _{1b1}	-2.78	0.91	-1.87
CR _{1a2-α}	-2.87	1.06	-1.81
CR _{1a2-β}	-2.70	0.75	-1.95
CR _{1b2-α}	-0.46	1.16	0.70
CR _{1b2-β}	-2.73	0.85	-1.88
CR _{1c2-β}	-2.93	0.85	-2.08
CR _{2a}	-2.78	0.81	-1.97
CR _{2b-α}	-2.19	1.00	-1.19
CR _{2b-β}	-2.44	1.27	-1.17
CR _{2b-γ}	-0.97	1.22	0.25
CP _{1a1}	-0.81	0.74	-0.07
CP _{1a2-α}	-0.92	0.81	-0.11
CP _{1a2-β}	-1.09	0.70	-0.39
CP _{1b2-α}	-2.01	0.78	-1.23
CP _{1b2-β}	-2.80	0.84	-1.96
CP _{1c2-β}	-1.58	0.91	-0.67
CP _{1c2-γ}	-2.16	0.86	-1.30
CP _{2a}	-1.45	0.72	-0.73
CP _{2b-α}	-3.01	0.88	-2.13
CP _{2b-β}	-2.95	0.88	-2.07
CP _{2b-γ}	-0.97	0.76	-0.21

(96.51 kcal mol^{-1}) and both of them are about 4 kcal mol^{-1} lower than $D_{298}^0(-\text{CH}_3)$ (99.61 kcal mol^{-1}). This result suggests that for reaction R1, channels R1a and R1b are more favorable than channel R1c. However, for $\text{CH}_3\text{CHClCH}_3$, the bond energies increase in the order $D_{298}^0(-\text{CHCl-})$ (94.33 kcal mol^{-1}) < $D_{298}^0(-\text{CH}_3)$ (100.13 kcal mol^{-1}), and the latter is larger than the former by about 6 kcal mol^{-1} at the BMC-CCSD//B3LYP level, which indicates that reaction R2 would proceed mainly via the H-abstraction from the chlorinated methylene (-CHCl-) position.

As the determination of the TS structure of a reaction is essential for the understanding of the reaction mechanism involved, the geometries of reaction channels R1b1, R1b2- β , and R2a, which are the major channels of reactions R1 and R2, respectively, are optimized at two levels, i.e., the B3LYP and BMK, with the 6-311G(d,p) basis set. The DFT has revolutionized the role of theory by providing accurate first-principles predictions of critical properties since its computational cost is low compared with *ab initio* methods. The B3LYP is an exceedingly popular functional developed more than 10 years ago, which has been demonstrated remarkably high performance/cost ratios for calculating accurate molecular structures. Over the past decade, a number of second-generation functionals have been developed that show great promises for improvement in both the calculation of reaction barrier heights and TS geometries. Among them, BMK can actually be considered a reliable general-purpose functional to describe the TS structure.^[27] Due to the system including oxygen and chlorine atoms, the geometries of above-mentioned three reaction channels are also optimized at the B3LYP and BMK levels with the 6-311+G(d,p) basis set. Then, the barrier heights are refined by several multicoefficient composite methods using different optimized geometries, respectively, as the accurate

Table 3. Calculated barrier heights (in kcal mol^{-1}) for R1b1, R1b2- β , and R2a by using various methods.

Levels	R1b1	R1b2- β	R2a
BMC-CCSD//BMK/6-311G(d,p)	-1.34	-1.40	-1.51
BMC-CCSD//BMK/6-311+G(d,p)	-1.10	-1.20	-0.92
BMC-CCSD//B3LYP/6-311G(d,p)	-0.70	-0.70	-0.44
BMC-CCSD//B3LYP/6-311+G(d,p)	-0.26	-0.38	-1.37
MCG3-MPWPW91//BMK/6-311G(d,p)	-0.63	-0.72	-0.75
MCG3-MPWPW91//BMK/6-311+G(d,p)	-0.47	-0.53	-0.33
MCG3-MPWPW91//B3LYP/6-311G(d,p)	-0.02	-0.04	0.09
MCG3-MPWPW91//B3LYP/6-311+G(d,p)	0.34	0.25	-0.94
MCQCISD-MPWPW91//BMK/6-311G(d,p)	-0.59	-0.65	-0.75
MCQCISD-MPWPW91//BMK/6-311+G(d,p)	-0.47	-0.50	-0.40
MCQCISD-MPWPW91//B3LYP/6-311G(d,p)	-0.002	-0.001	0.12
MCQCISD-MPWPW91//B3LYP/6-311+G(d,p)	0.35	0.29	-0.83

determination of the magnitude of the barrier height is vital in the study of the kinetics or dynamics of a reaction. The corresponding results are listed in Table 3. First, the barrier heights refined by the same composite method on the different geometries are investigated. The different geometries mean two situations: one is that the geometries are calculated by the same level with the different basis set; the other is that the structures are optimized by the different levels, i.e., BMK and B3LYP, with the same basis set. As can be seen from Table 3, the barrier heights refined by the same composite method on the different geometries show well consistent with the maximum error within 1 kcal mol^{-1} . So, the geometries optimized by the B3LYP functional with the 6-311G(d,p) basis set are reliable in this study. Let us turn our attention to the barrier heights refined by different composite methods. The values obtained at the three higher levels, i.e., BMC-CCSD, MCQCISD-MPWPW91, and MCG3-MPWPW91, based on the same geometries show good mutual agreement, which indicates that the BMC-CCSD//B3LYP/6-311G(d,p) method is a reliable choice to refine the energies for these systems. Thus, in this study, we use the BMC-CCSD//B3LYP/6-311G(d,p) method to refine the potential energy surface and to calculate the rate constants.

Dynamics calculations

Dual-level (X/Y) direct dynamics calculations are performed for these reactions by using the VTST-ISPE^[29] approach. The rate constants for each reaction channel are evaluated by using the conventional transition-state theory (TST) and CVT over a wide temperature range of 200-2000 K. Tunneling is corrected by means of the small-curvature tunneling (SCT) correction.

As the reaction channels R1a1 and R1c1- β are more favorable reaction channels, these two reaction channels are selected as the representatives to analyze the variational and tunneling effect. Plots of the TST, CVT, and CVT/SCT rate constants of channels R1a1 and R1c1- β as functions of the reciprocal of the temperature are presented in Figures 3a-3b, respectively. It can be found that for channel R1a1, the TST and CVT rate constants are nearly the same over a whole temperature range, which indicates that the variational effect on the rate constants is very small or almost negligible over the whole

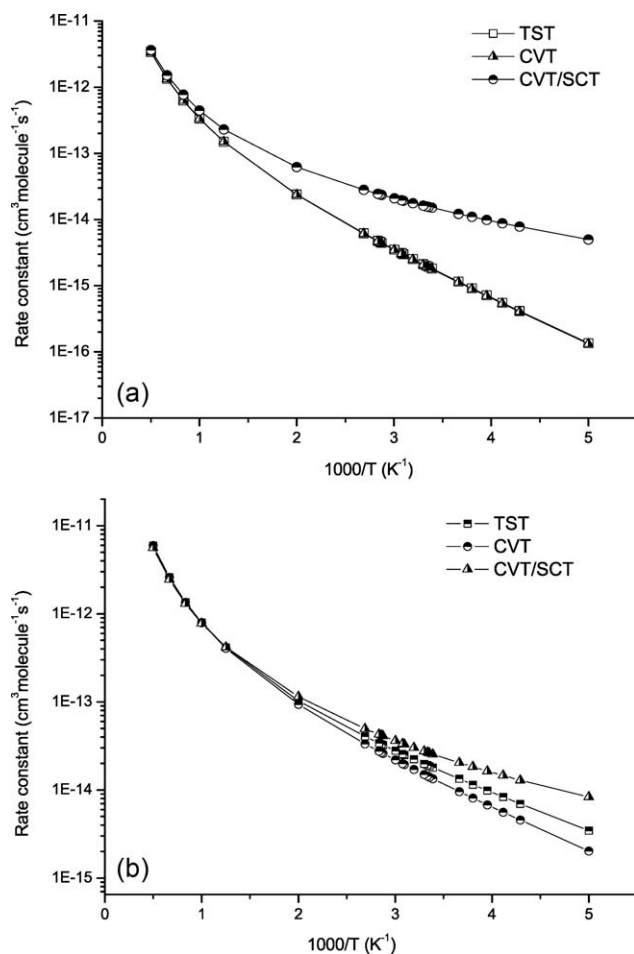


Figure 3. a) Plot of the TST, CVT, and CVT/SCT rate constants calculated at the BMC-CCSD//B3LYP/6-311G(d,p) level versus $1000/T$ between 200 and 2000 K for the reaction $\text{CH}_3\text{CH}_2\text{CH}_2\text{Cl} (\text{SC}_1) + \text{OH} \rightarrow \text{CH}_3\text{CH}_2\text{CHCl} (\text{P}_{1a1}) + \text{H}_2\text{O}$ (R1a1). b) Plot of the TST, CVT, and CVT/SCT rate constants calculated at the BMC-CCSD//B3LYP/6-311G(d,p) level versus $1000/T$ between 200 and 2000 K for the reaction $\text{CH}_3\text{CH}_2\text{CH}_2\text{Cl} (\text{SC}_1) + \text{OH} \rightarrow \text{CH}_2\text{CH}_2\text{CH}_2\text{Cl} (\text{P}_{1c1}) + \text{H}_2\text{O}$ (R1c1- β).

calculated temperature range. However, for channel R1c1- β , the ratio between CVT and TST rate constants ranges from a value of 0.59 at 200 K to a value of 0.99 at 1000 K. Thus, the variational effect should be taken into account at lower temperatures. With temperature increasing, the TST values are almost the same with the CVT ones, implying that variational effect can be negligible at higher temperatures. Other H-abstraction reaction channels are similar to channel R1c1- β . To analyze this behavior in more detail, the classical potential energy curve ($V_{\text{MEP}}(s)$), the vibrationally adiabatic ground-state potential energy curve ($V_a^G(s)$), and the ZPE curve for the reaction channels R1a1 and R1c1- β as a function of the IRC(s) are plotted in Figures 4a–4b, respectively. The maximum of the potential energy profile at the BMC-CCSD//B3LYP level is slightly shifted in the s direction for both reaction channels, which is the case that the saddle point position of the dual-level is generally shifted with the VTST-ISPE scheme.^[29] For reaction R1a1, the positions of the maximum values of the $V_{\text{MEP}}(s)$ and $V_a^G(s)$ curves are located at the same position, i.e.,

around $s = 0.09$ bohr. However, for the channel R1c1- β , the locations of the maximum values of the $V_{\text{MEP}}(s)$ and $V_a^G(s)$ curves shift toward the reactants to approximately -0.09 and -0.27 bohr, respectively. So, the variational effect is small in evaluating the rate constants for channel R1a1 and is larger for channel R1c1- β . By contrasting the CVT and CVT/SCT, the CVT/SCT rate constants are quite larger than those of CVT, especially at low-temperature range. The ratios of $k_{\text{CVT/SCT}}/k_{\text{CVT}}$ are 38 and 4.1 at 200 K for channels R1a1 and R1c1- β , respectively. Thus, SCT correction plays an important role at lower temperatures.

Two conformers are located for $\text{CH}_3\text{CH}_2\text{CH}_2\text{Cl}$ and the energy of SC_1 is very close to that of SC_2 , so both conformers will contribute to the overall reaction rate constants. The total rate constant (k_1) for this reaction can be obtained from the following expression: $k_1 = \omega_1 k_{\text{sc1}} + \omega_2 k_{\text{sc2}} = \omega_1 (k_{1a1} + k_{1b1} + k_{1c1-\alpha} + k_{1c1-\beta}) + \omega_2 (k_{1a2-\alpha} + k_{1a2-\beta} + k_{1b2-\alpha} + k_{1b2-\beta} + k_{1c2-\alpha} + k_{1c2-\beta} + k_{1c2-\gamma})$ (1) where ω_1 and ω_2 are the weight factors of

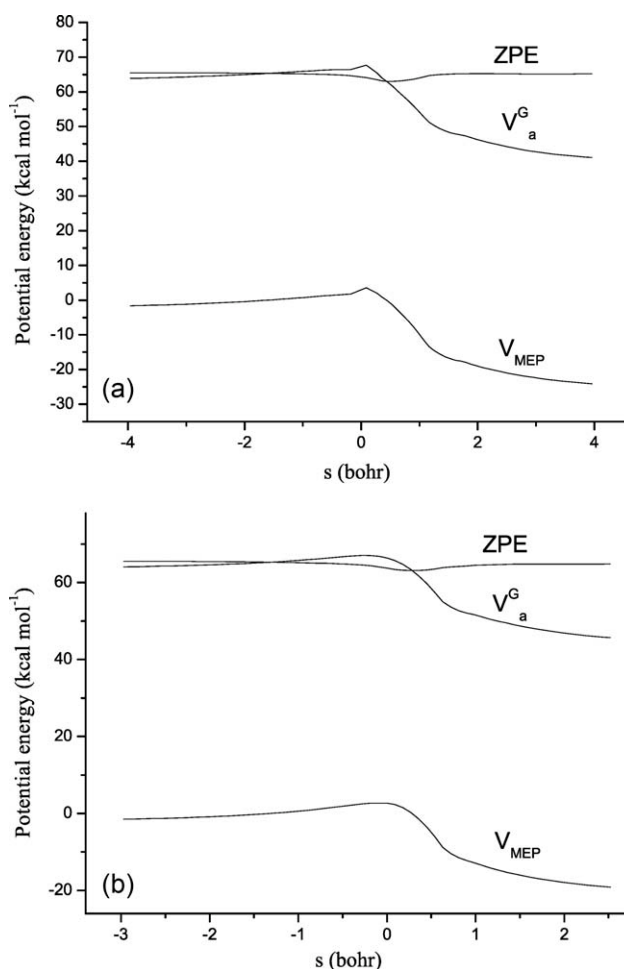


Figure 4. a) Classical potential energy curve (V_{MEP}), ground-state vibrationally adiabatic energy curve (V_a^G), and ZPE curve as functions of s (bohr) at the BMC-CCSD//B3LYP/6-311G(d,p) level for the reaction $\text{CH}_3\text{CH}_2\text{CH}_2\text{Cl} (\text{SC}_1) + \text{OH} \rightarrow \text{CH}_3\text{CH}_2\text{CHCl} (\text{P}_{1a1}) + \text{H}_2\text{O}$ (R1a1). b) Classical potential energy curve (V_{MEP}), ground-state vibrationally adiabatic energy curve (V_a^G), and ZPE curve as functions of s (bohr) at the BMC-CCSD//B3LYP/6-311G(d,p) level for the reaction $\text{CH}_3\text{CH}_2\text{CH}_2\text{Cl} (\text{SC}_1) + \text{OH} \rightarrow \text{CH}_2\text{CH}_2\text{CH}_2\text{Cl} (\text{P}_{1c1}) + \text{H}_2\text{O}$ (R1c1- β).

each conformer calculated from the Boltzmann distribution function, k_{1a1} , k_{1b1} , $k_{1c1-\alpha}$, $k_{1c1-\beta}$, $k_{1a2-\alpha}$, $k_{1a2-\beta}$, $k_{1b2-\alpha}$, $k_{1b2-\beta}$, $k_{1c2-\alpha}$, $k_{1c2-\beta}$, and $k_{1c2-\gamma}$ are the separate rate constants of each reaction channel, and $k_{\text{SC}1}$ and $k_{\text{SC}2}$ are the sum rate constants for the hydrogen abstraction from the SC_1 and SC_2 isomers of $\text{CH}_3\text{CH}_2\text{CH}_2\text{Cl}$. It should be noted that the weight factors ω_1 and ω_2 are temperature dependence. The values of ω_1 are 0.45 at 200 K and 0.49 at 1000 K. Thus, it is easy to evaluate what degree each conformer contributes to the total rate constants. Because the barrier heights of channels R1b1 and R1b2- β are negative, the tunneling correction is not included for these two channels. The k_{1b1} and $k_{1b2-\beta}$ are the CVT rate constants, while all other reaction channels in the expression (1) are the CVT/SCT rate constants. And because SC_1 is C_s symmetry, the symmetry factor $\sigma = 2$ for the reaction channels R1a1, R1b1, and R1c1- β is considered in the rate constant calculation.

The temperature dependence of the rate constants of channels R1a, R1b, R1c, and the total rate constants are presented in Figure 5a, as well as the corresponding experimental and

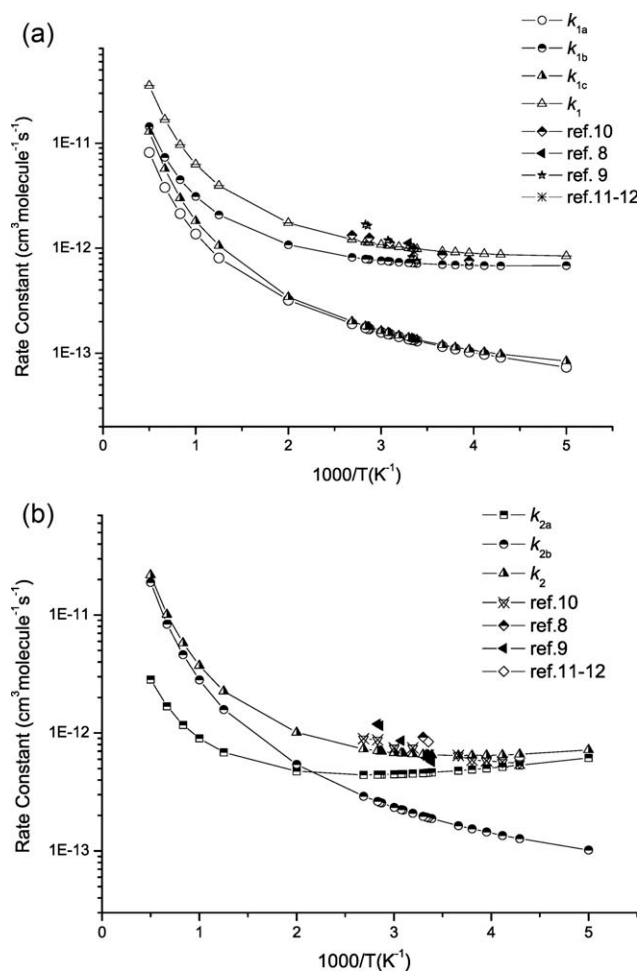


Figure 5. a) Plot of the total rate constants calculated at the BMC-CCSD//B3LYP/6-311G(d,p) level along with the available experimental values versus $1000/T$ between 200 and 2000 K for the reaction $\text{CH}_3\text{CH}_2\text{CH}_2\text{Cl} + \text{OH}$ (R1). b) Plot of the total rate constants calculated at the BMC-CCSD//B3LYP/6-311G(d,p) level along with the available experimental values versus $1000/T$ between 200 and 2000 K for the reaction $\text{CH}_3\text{CHClCH}_3 + \text{OH}$ (R2).

theoretical values. Three experimental and one theoretical studies were made for the reaction $\text{CH}_3\text{CH}_2\text{CH}_2\text{Cl} + \text{OH} \rightarrow$ products (R1). The slope of the results reported by Markert and Nielsen^[9] are larger than that measured by Mu et al.^[10] Moreover, the rate constant reported by Markert and Nielsen^[9] is lower than other values at room temperature. Other values measured or estimated by three different groups agree well with each other. The calculated rate constants of reaction R1 are in excellent agreement with the available experimental values in the measured temperature range of 253–372 K.^[8–10] The deviation between the calculated and experimental values remains within a factor of approximately 0.8 to 1.5. Moreover, the activation energy of 0.47 kcal mol⁻¹ (253–372 K) agrees well with the corresponding experimental result of 1.05 ± 0.1 kcal mol⁻¹.^[10] However, the activation energy of 0.54 kcal mol⁻¹ (295–353 K) is lower than that of 2.86 ± 1.0 kcal mol⁻¹ reported by Markert and Nielsen.^[9] These three groups also studied the reaction R2 and got the corresponding rate constants.^[8–10] Similarly, the values obtained by Markert's group^[9] are different from other ones. In the case of $\text{CH}_3\text{CHClCH}_3$, only one conformer is located, so the total rate constants for reaction $\text{CH}_3\text{CHClCH}_3$ with OH radical are obtained from the sum of the individual rate constants $k_2 = k_{2a} + k_{2b-\alpha} + k_{2b-\beta} + k_{2b-\gamma}$, which are plotted in Figure 5b. Because the two $-\text{CH}_3$ groups are identity, the symmetry factor $\sigma = 2$ is taken into account for the channels R2b (including R2b- α , R2b- β , and R2b- γ). The agreement between calculated results and experimental ones is seen to be remarkably good. The ratios of $k_{(\text{expt.})}/k_2$ remain within a factor of approximately 0.9 to 1.7 in a temperature range of 233–372 K. The activation energy of 0.12 kcal mol⁻¹ (233–372 K) is slightly lower than the corresponding experimental result of 0.73 ± 0.13 kcal mol⁻¹.^[10] However, in the temperature range of 295–353 K, the difference between the calculated and experimental result^[9] is larger (0.28 vs. 2.63 ± 1.67 kcal mol⁻¹).

To further study the mechanisms of hydrogen abstraction reactions $\text{CH}_3\text{CH}_2\text{CH}_2\text{Cl} + \text{OH}$ and $\text{CH}_3\text{CHClCH}_3 + \text{OH}$, the temperature dependence of branching ratios for the two reactions is exhibited in Figures 6a and 6b, respectively. For the reaction $\text{CH}_3\text{CH}_2\text{CH}_2\text{Cl} + \text{OH}$ (R1), as shown in Figure 6a, k_{1b} is about 1 order larger than k_{1a} and k_{1c} , and the total rate constants are nearly equal to the rate constants of reaction R1b. Thus, channel R1b (H-abstraction from $-\text{CH}_2-$ group) prefers in the lower temperature. However, the contribution of k_{1c} to the total rate constants increases with the temperature increasing. With respect to reaction $\text{CH}_3\text{CHClCH}_3 + \text{OH}$ (R2), the channel R2a (H-abstraction from $-\text{CHCl}-$ group) dominates the reaction R2 below 400 K. However, the channel R2b (H-abstraction from $-\text{CH}_3$ group) gradually becomes more important in the higher temperatures and exceeds channel R2a to the major channel.

Owing to the good agreement between the theoretical and experimental values, it is reasonable to believe that the present calculations can provide reliable predictions of the rate constants for the title reactions during a large temperature region, which will be useful for the atmospheric modeling calculations and help to assess their atmospheric lifetimes. Thus,

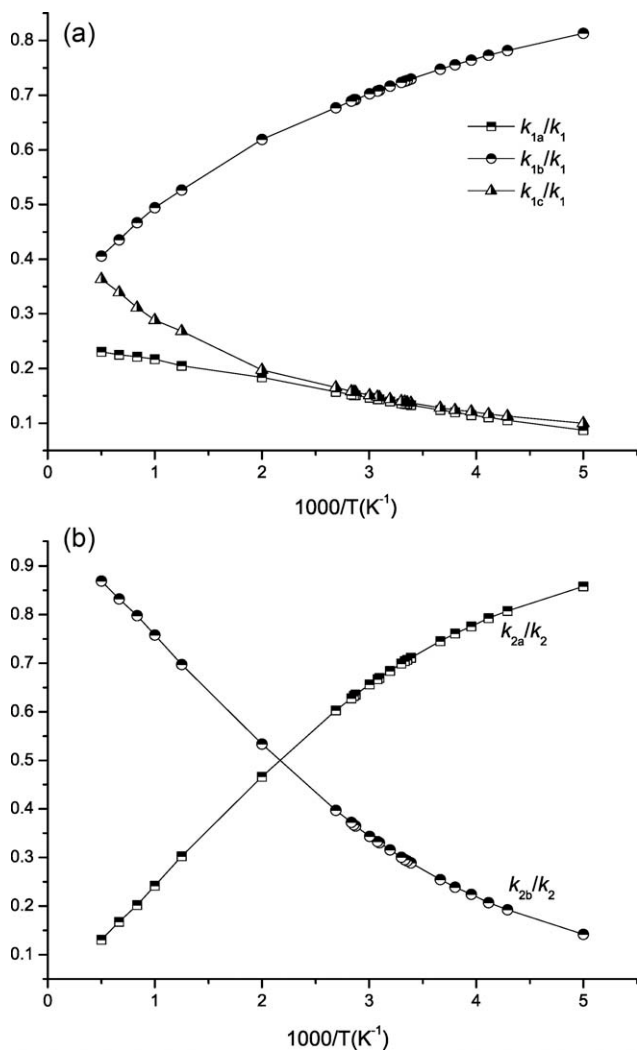


Figure 6. a) Plot of the calculated branching ratio versus $1000/T$ between 200 and 2000 K for the $\text{CH}_3\text{CH}_2\text{CH}_2\text{Cl} + \text{OH}$ (R1). b) Plot of the calculated branching ratio versus $1000/T$ between 200 and 2000 K for the $\text{CH}_3\text{CHCICH}_3 + \text{OH}$ (R2).

for the convenience of future experimental measurements, the total rate constants of R1 and R2 are firstly fitted to the popular modified Arrhenius expression, $k = AT^n \exp(-E/RT)$, where A , n , and E are fitting parameters and R is the gas constant. This equation is labeled model 1 in this article. Model 1 has been used widely for fitting theoretical rate constants in the literatures.^[47–49] Recently, Zheng and Truhlar^[50] proposed a new model with one more parameter to give small fitting error and have the correct low-temperature asymptotic behavior for activation energy and rate constant, which is called model 2. The model 2 rate constant expression is $k = AT^n \exp[-E(T+T_0)/R(T^2+T_0^2)]$, where A , n , E , and T_0 are fitting parameters and R is the gas constant. The fitting results are presented in Table 4. For both reactions, the fitting errors of model 2 are smaller than those of model 1 over whole temperatures. The model 2 should be recommended for fitting since it gives very small fitting errors for the reactions studied in this work and other references.^[50,51] To illustrate the discrepancy caused by fitted models, we plot the rate constants

Table 4. The fitted parameters using two modified Arrhenius equations for reactions R1 and R2 in a temperature range from 200 K to 2000 K.

	R1	R2
Model 1		
$k = AT^n \exp(-E/RT)$		
A (s ⁻¹)	1.61×10^{-20}	8.62×10^{-22}
n	2.78	3.09
E (kcal mol ⁻¹)	-1.23	-1.67
RMSR	0.03	0.023
Model 2		
$k = AT^n \exp[-E(T+T_0)/R(T^2+T_0^2)]$		
A (s ⁻¹)	4.16×10^{-21}	8.05×10^{-22}
n	2.97	3.11
E (kcal mol ⁻¹)	-1.17	-1.37
T_0 (K)	124.6	106.4
RMSR	0.02	0.016

k_1 and k_2 fitted by the model 1 and model 2 in Figures 7a and 7b, respectively. Model 2 clearly provides a better low-temperature asymptotic behavior, which is very important to generate accurate rate constants at any temperature within the range that is used in the fitting and to extrapolate the rate constants beyond the temperature range that used in the fitting.

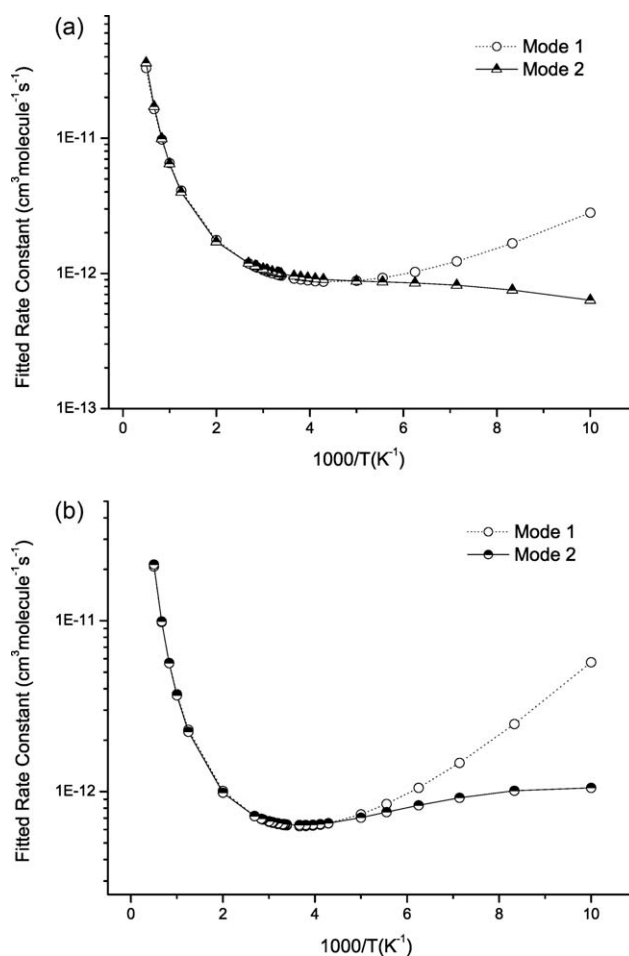


Figure 7. a) Plot of the rate constants versus $1000/T$ fitted by Model 1 and Model 2 for R1. b) Plot of the rate constants versus $1000/T$ fitted by Model 1 and Model 2 for R2.

Conclusion

In this article, the hydrogen abstraction reactions of $\text{CH}_3\text{CH}_2\text{CH}_2\text{Cl}$ (R1) and $\text{CH}_3\text{CHClCH}_3$ (R2) with OH radicals are studied by dual-level direct dynamics method. Dynamics calculations are performed by using the VTST-ISPE at the BMC-CCSD//B3LYP/6-311G(d,p) level. The small-curvature tunneling effect plays an important role in a lower temperature range for all the reaction channels with the positive barrier heights, while the variational effect is small and negligible for some reaction channels. For reactions OH radicals with $\text{CH}_3\text{CH}_2\text{CH}_2\text{Cl}$ (R1) and $\text{CH}_3\text{CHClCH}_3$ (R2), the channels of H-abstraction from $-\text{CH}_2-$ and $-\text{CHCl}$ groups are the major reaction channels, respectively, at lower temperatures. The agreement between calculated and experimental rate constants is seen to be remarkably good. On the other hand, the values of enthalpies of formation for $\text{CH}_3\text{CHCH}_2\text{Cl}$, $\text{CH}_2\text{CH}_2\text{CH}_2\text{Cl}$, and $\text{CH}_3\text{CHClCH}_2$ species are calculated at the BMC-CCSD//B3LYP/6-311G(d,p) level by isodesmic reactions. Finally, the total rate constants are fitted by two models, i.e., three-parameter and four-parameter expressions over a wide temperature range of 200–2000 K. Four-parameter expression is recommended because it gives smaller fitting errors and provides a better low-temperature asymptotic behavior.

Acknowledgments

The authors thank Professor Donald G. Truhlar for providing the POLYRATE 9.7 program and the State Key Laboratory of Physical Chemistry of Solid Surfaces for providing computational resources.

- [1] R. Atkinson, *J Phys Chem Ref Data* 1994, Monograph. No. 2.
- [2] WMO, Global Ozone Research and Monitoring Project, Report No 37, Scientific Assessment of Ozone Depletion, 1994.
- [3] C. Hubrich, F. Stuhl, *J Photochem* 1980, 12, 93.
- [4] L. N. Krasnoperov, J. V. Michael, *J Phys Chem A* 2004, 108, 5643.
- [5] G. Bravo-Perez, J. R. Alvarez-Idaboy, A. G. Jimenez, A. Cruz-Torres, *Chem Phys* 2005, 310, 213.
- [6] S. N. Kozlov, V. L. Orkin, M. J. Kurylo, *J Phys Chem A* 2003, 107, 2239.
- [7] S. C. Herndon, T. Gierczak, R. K. Talukdar, A. R. Ravishankara, *Phys Chem Chem Phys* 2001, 3, 4529.
- [8] T. Donaghy, I. Shanahan, M. Hande, S. Fitzpatrick, *Int J Chem Kinet* 1993, 25, 273.
- [9] F. Markert, O. J. Nielsen, *Chem Phys Lett* 1992, 194, 123.
- [10] Y. J. Mu, A. Mellouki, *Phys Chem Chem Phys* 2001, 3, 2614.
- [11] R. Atkinson, *Int J Chem Kinet* 1987, 19, 799.
- [12] E. S. C. Kwok, R. Atkinson, *Atmos Environ* 1995, 29, 1685.
- [13] D. G. Truhlar, In *The Reaction Path in Chemistry: Current Approaches and Perspectives*, D. Heidrich, Eds.; Kluwer: Dordrecht, 1995; p 229.
- [14] D. G. Truhlar, B. C. Garrett, S. J. Klippenstein, *J Phys Chem* 1996, 100, 12771.
- [15] W. P. Hu, D. G. Truhlar, *J Am Chem Soc* 1996, 118, 860.
- [16] W. P. Hu, Y. P. Liu, D. G. Truhlar, *J Chem Soc Faraday Trans* 1994, 90, 1715.
- [17] J. C. Corchado, E. L. Coitiño, Y. Y. Chang, P. L. Fast, D. G. Truhlar, *J Phys Chem A* 1998, 102, 2424.
- [18] J. C. Corchado, Y. Y. Chuang, P. L. Past, W. P. Hu, Y. P. Liu, G. C. Lynch, K. A. Nguyen, C. F. Jackels, A. Fernandez-Ramos, B. A. Ellingson, B. J. Lynch, J. J. Zheng, V. S. Melissas, J. Villa, I. Rossi, E. L. Coitiño, J. Z. Pu, T. V. Albu, R. Steckler, B. C. Garrett, A. D. Isaacson, D. G. Truhlar, POLYRATE, version 9.7, University of Minnesota, Minneapolis, 2007.
- [19] D. G. Truhlar, B. C. Garrett, *Acc Chem Res* 1980, 13, 440.
- [20] D. G. Truhlar, A. D. Isaacson, B. C. Garrett, In *The Theory of Chemical Reaction Dynamics*, M. Baer, Ed.; CRC Press: Boca Raton, 1985; p. 65.
- [21] D. G. Truhlar, B. C. Garrett, *Annu Rev Phys Chem* 1984, 35, 159.
- [22] Gaussian 09, Revision A.1, M. J. Frisch, G. W. Trucks, H. B. Schlegel, G. E. Scuseria, M. A. Robb, J. R. Cheeseman, G. Scalmani, V. Barone, B. Men- nucci, G. A. Petersson, H. Nakatsuji, M. Caricato, X. Li, H. P. Hratchian, A. F. Izmaylov, J. Bloino, G. Zheng, J. L. Sonnenberg, M. Hada, M. Ehara, K. Toyota, R. Fukuda, J. Hasegawa, M. Ishida, T. Nakajima, Y. Honda, O. Kitao, H. Nakai, T. Vreven, J. A. Montgomery, Jr., J. E. Peralta, F. Ogliaro, M. Bear- park, J. J. Heyd, E. Brothers, K. N. Kudin, V. N. Staroverov, R. Kobayashi, J. Normand, K. Raghavachari, A. Rendell, J. C. Burant, S. S. Iyengar, J. Tomasi, M. Cossi, N. Rega, N. J. Millam, M. Klene, J. E. Knox, J. B. Cross, V. Bakken, C. Adamo, J. Jaramillo, R. Gomperts, R. E. Stratmann, O. Yazyev, A. J. Austin, R. Cammi, C. Pomelli, J. W. Ochterski, R. L. Martin, K. Morokuma, V. G. Zakrzewski, G. A. Voth, P. Salvador, J. J. Dannenberg, S. Dapprich, A. D. Daniels, Ö. Farkas, J. B. Foresman, J. V. Ortiz, J. Cioslowski, D. J. Fox, Gaus- sian, Inc., Wallingford, CT, 2009.
- [23] A. D. Becke, *J Chem Phys* 1993, 98, 1372.
- [24] C. Lee, W. Yang, R. G. Parr, *Phys Rev B* 1998, 37, 785.
- [25] B. J. Lynch, Y. Zhao, D. G. Truhlar, *J Phys Chem A* 2005, 109, 1643.
- [26] S. F. Boys, F. Bernardi, *Mol Phys* 1970, 19, 553.
- [27] A. D. Boese, J. M. L. Martin, *J Chem Phys* 2004, 121, 3405.
- [28] Y. Zhao, B. J. Lynch, D. G. Truhlar, *Phys Chem Chem Phys* 2005, 7, 43.
- [29] Y. Y. Chuang, J. C. Corchado, D. G. Truhlar, *J Phys Chem* 1999, 103, 1140.
- [30] B. C. Garrett, D. G. Truhlar, *J Chem Phys* 1979, 70, 1593.
- [31] B. C. Garrett, D. G. Truhlar, *J Am Chem Soc* 1979, 101, 4534.
- [32] B. C. Garrett, D. G. Truhlar, R. S. Grev, A. W. Magnuson, *J Phys Chem* 1980, 84, 1730.
- [33] D. H. Lu, T. N. Truong, V. S. Melissas, G. C. Lynch, Y. P. Liu, B. C. Garrett, R. Steckler, A. D. Isaacson, S. N. Rai, G. C. Hancock, J. G. Lauderdale, T. Joseph, D. G. Truhlar, *Comput Phys Commun* 1992, 71, 235.
- [34] Y. P. Liu, G. C. Lynch, T. N. Truong, D. H. Lu, D. G. Truhlar, B. C. Garrett, *J Am Chem Soc* 1993, 115, 2408.
- [35] J. R. Daring, X. Zhu, S. Shen, *J Mol Struct* 2001, 570, 1.
- [36] D. R. Lide, *CRC Handbook of Chemistry and Physics*, 80th ed.; CRC Press: New York, 1999.
- [37] M. Meyer, J. U. Grabow, H. Dreizler, *J Mol Spectrosc* 1992, 151, 217.
- [38] K. Yamanouchi, M. Sugie, H. Takeo, C. Matsumura, K. Kuchitsu, *J Phys Chem* 1984, 88, 2315.
- [39] M. W. Chase, Jr. *J Phys Chem Ref Data*, 1998, Monograph 9, 1.
- [40] W. Tsang, In *Energetics of Organic Free Radicals*, J. A. Martinho Simoes, A. Greenberg, J. F. Liebman, Eds.; Blackie Academic and Professional: London, 1996; pp. 22–58.
- [41] R. A. Fletcher, *Trans Faraday Soc* 1971, 67, 3191.
- [42] Y. R. Luo, *Comprehensive Handbook of Chemical Bond Energies*, CRC Press: Boca Raton, FL, 2007.
- [43] W. B. DeMore, S. P. Sander, S. P. Golden, C. J. Howard, D. M. Golden, C. E. Kolb, R. F. Hampson, M. J. Molina, *Chemical Kinetics and Photochemical Data for Use in Stratospheric Modeling*, NASA: Pasadena, California, 1997.
- [44] B. Ruscic, D. Feller, D. A. Dixon, K. A. Peterson, L. B. Harding, R. L. Asher, A. F. Wagner, *J Phys Chem A* 2001, 105, 1.
- [45] J. A. Joens, *J Phys Chem A* 2001, 105, 11041.
- [46] B. Ruscic, A. F. Wagner, L. B. Harding, R. L. Asher, D. Feller, D. A. Dixon, K. A. Peterson, Y. Song, X. Qian, C. Y. Ng, J. Liu, W. Chen, D. W. Schwenke, *J Phys Chem A* 2002, 106, 2727.
- [47] H. X. Liu, Y. Wang, L. Yang, J. Y. Liu, H. Gao, Z. S. Li, C. C. Sun, *J Com- put Chem* 2009, 30, 2194.
- [48] H. Gao, Y. Wang, S. Q. Wan, J. Y. Liu, C. C. Sun, *J Mol Struct-Theochem* 2009, 913, 107.
- [49] L. Wang, Y. Zhao, J. Zhang, Y. N. Dai, J. L. Zhang, *Theor Chem Acc* 2011, 128, 183.
- [50] J. J. Zheng, D. G. Truhlar, *Phys Chem Chem Phys* 2010, 12, 7782.
- [51] L. Wang, Y. Zhao, J. L. Zhang, *J Fluorine Chem* 2011, 132, 216.

Received: 24 March 2011

Revised: 22 July 2011

Accepted: 16 August 2011

Published online on 26 September 2011